

Harmonic Phase Flow for Tissue Motion Estimation in Tagged MR Sequences

J Garcia-Barnes¹, D Gil¹, J Barajas^{1,2}, F Carreras³, S Pujadas³ and P Radeva¹

¹ *Computer Vision Center, Universitat Autònoma de Barcelona, Bellaterra, Spain*

² *CICATA-IPN, Queretaro, Mexico*

³ *Hospital de la Sta Creu i St Pau, Barcelona, Spain*

E-mail: jaumegb@cvc.uab.es

Abstract In this work, we present a fully automated method for tissue deformation estimation in tagged magnetic resonance images (TMRI). The method consists of two main stages: in the first one, we use Gabor filter banks, tuned independently for each left ventricle level, that allows to obtain optimally filtered complex images the phase of which is a property that remains constant along the cardiac cycle. This fact can be thought as the brightness constancy condition required by classical optical flow (OF) methods. Pairs of these filtered sequences, together to a variational formulation are used in a second step with obtain dense continuous deformation map that we call Harmonic Phase Flow.

This method has been used to determine reference values of ventricular torsion (VT) in a set of 8 healthy volunteers. The results encourage the use of VT as a useful parameter for ventricular function assessment in clinical routine.

1 Introduction

The cardiac function is a complex mechanism, composed mainly by contraction and rotation of the myocardium, which is the precise result of the electro-mechanical activation of the ventricular band [1]. This band is double twisted in a fashion that determines the two main chambers of the heart: the left and the right ventricle. Although any cardiovascular disease may affect locally the myocardial tissue, this could expand to the whole heart function, causing exercise tolerance impairment or even death. Clinical assessment of patient symptoms passes through a complete analysis of the global and also regional function of the heart.

Currently, there are many imaging techniques that

allow the visualization of cardiac function. Nevertheless, Tagged MRI [2] is the reference imaging modality for regional assessment of the heart function. This technique produces a grid like pattern of saturated magnetization (using any of the available tagging protocols: SPAMM, CSPAMM or DANTE, prior to any cardiac ordinary MRI sequence) over the myocardium (Fig. 1.a) that deforms by the underlying motion of the heart, allowing the visualization of transmural deformation.

Since the appearance of Tagged MRI, in the late 80's, many analysis techniques have been developed in order to extract motion data. We differentiate three main categories. The first one consider the dark stripes as target features to be tracked ([3]). One of their problems is due to the so called fading effect, in virtue of which, contrast between tissue and tags diminishes in time. Other authors [4] use more robust techniques to avoid this negative effect. Nevertheless, they all share an additional problem. They lead sparse displacement fields that have to be further interpolated. The second category consists of OF-based techniques [5] that overcome this last limitation, as they provide dense motion fields. However, they are still sensible to the fading effect, as they are based on the brightness constraint equation. For this reason, several authors have either suppressed this effect [6] or modelled its brightness variation [7].

All the previous methods share the property that they are applied in the spatial domain. On the third side we have the spectral or harmonic phase-based (HARP) methods [8] which are applied in the frequency domain. They rely on the fact that phase is property of the tissue that remains constant along the cardiac cycle [8]. For this reason, they can be

thought as an optical flow technique in a domain where brightness constancy is guaranteed. Although HARP methods are very fast, they cannot deal with large tissue deformation such those occurred at end-systole. Moreover, HARP-tracking is performed individually on each point, leading to discontinuous deformation maps. Hence, some authors have used regularization methods, either in the spatial [9] or in the frequency [10] domain.

Tagging studies are still not used in the clinical routine. This is due to two factors: (1) lack of reference values for new data derived from such imaging modality (stress, strain, torsion) and (2) lack of a commercial software capable of dealing efficiently with the great amount of data provided by the tagging studies. In the present work we develop a regularized spectral optical flow method, under a variational framework that uses banks of Gabor filters. We call it *Harmonic Phase Flow* and we apply it to the characterization of ventricular torsion in healthy subjects.

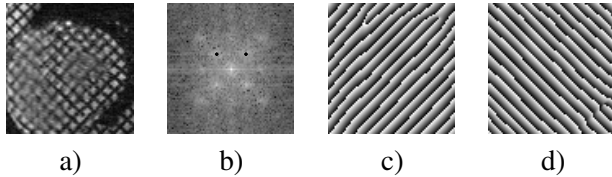


Figure 1: a) Frame of a Tagged MR sequence. b) Its Fourier Transform with two linearly independent harmonic peaks selected (ω_1, ω_2). c) and d) HARP images (a_1, a_2) associated to the selected harmonic peaks.

2 HARP images & HARP-tracking

The SPAMM tagging protocol [2] "prints" over the myocardium, two sets of linearly independent tags (Fig. 1.a) with main frequencies (ω_1, ω_2) that produce K spectral harmonic peaks in the frequency domain (Fig. 1.b), depending on the desired profile of the tags. This fact makes any tagged frame to have the form $I(x, y; t) = \sum_{k=1}^K I_k(x, y; t)$ [8] with

$$I_k(x, y; t) = I_0(p(x, y; t))c_k(t)e^{i\omega_k p(x, y; t)} \quad (1)$$

where $p(x, y; t)$ is the reference map that relates a spatial point (x, y) at time t to its associated material point at time $t = 0$; I_0 is underlying ordinary MR

image (without tags) and c_k is a function of time that reflects the fading effect.

Each I_k corresponds to one of the mentioned harmonic peaks and their phase, $\Phi_k(x, y; t) = \omega_k p(x, y; t)$, is a stable property of the tissue, as it linearly depends on the reference map [8]. In practice, the phase cannot be retrieved, instead its principal wrapped value, $a_k = \angle(\Phi_k) \in [-\pi, \pi)$, is obtained. This is called HARP image (Fig. 1.c and .d) and it provides motion information in a direction close to ω_k . In order to extract 2D motion, two HARP images associated with linearly independent harmonic peaks are required $\{a_1, a_2\}$.

At each instant t , one can associate to each point in the frame, a couple of angle values $a(x, y; t) = [a_1(x, y; t), a_2(x, y; t)]$. HARP tracking [14] is an algorithm that estimates tissue motion assuming that if a material point $(x^t, y^t; t)$ has $[a_1, a_2]$ values, this material point in the next frame $(x^{t+1}, y^{t+1}; t + 1)$ must have the same angle values due to the phase constancy. Dense deformation maps (Fig. 4.a) are obtained by solving independently for each point the following nonlinear system:

$$a(x, y, t + 1) - a(x^t, y^t, t) = 0 \quad (2)$$

When a tagged frame is given, all the I_k 's are mixed. In order to isolate any of them, its associated harmonic peak is filtered. In [11], they use elliptical bandpass regions with a gaussian rolloff outside. Although this method is simple, fast, and works well in early stages of systole, it may fail if deformation of tissue is not homogenous or when large deformations occur, as it is a relatively global operation. Other authors ([12], [13]) have used banks of Gabor filters aiming to overcome this drawback. Their potential relies on the spatial domain, where the multiple parameters can be tuned in order to fit the tissue, leading to more accurate estimates of the HARP images.

3 Classical optical flow

Although there are many optical flow techniques, in this section we will focus on that of [15] which can be defined as a global differential method. It relies on the hypothesis that intensity structures of local time-varying image regions are approximately constant, which is formalized as $I(x, y; t) \simeq I(x + \delta x, y +$

$\delta y; t + \delta t$). Taylor development of the second term yields the *optical flow constraint equation*:

$$\nabla I \cdot V + I_t = 0 \quad (3)$$

where $\nabla I = (I_x, I_y)$ is the image gradient and $V(x, y) = (u(x, y), v(x, y))$ is the image velocity. Notice that while we have two unknowns (u and v), only one equation (3) is available. This fact, that determines an infinity number of solutions, is known as *aperture problem*. To overcome this drawback, equation (3) is used in conjunction with a regularization term in a variational framework:

$$\varepsilon = \int \int (\alpha^2 \varepsilon_{reg}^2 + \varepsilon_{data}^2) dx dy \quad (4)$$

where $\varepsilon_{reg} = (\frac{\partial u}{\partial x})^2 + (\frac{\partial v}{\partial y})^2 + (\frac{\partial u}{\partial y})^2 + (\frac{\partial v}{\partial x})^2$ imposes smoothness conditions and $\varepsilon_{data} = I_x u + I_y v + I_t$ is given by (3). The minimizer of equation (4) is the desired optical flow field.

4 Harmonic phase flow

In general, constancy of brightness is not met in arbitrary sequences. This fact makes the previous OF method not to be suitable in most cases. Thus, we propose not to apply OF directly over the input Tagged MR sequences, but over phase sequences derived from them and which have been proven to maintain their values constant in time.

In order to obtain phase images Φ_1 and Φ_2 , first we have to compute I_1 and I_2 . To do so, we use Gabor filters given by:

$$\Gamma(x, y) = C e^{-i2\pi(\frac{\eta_x x}{W} + \frac{\eta_y y}{H})} \cdot e^{-\frac{(x')^2 + (\lambda y')^2}{2\sigma_{x'}}} \quad (5)$$

where $x' = x \cos \phi + y \sin \phi$ and $y' = -x \sin \phi + y \cos \phi$ establish the rotation of the Gaussian envelope, $\sigma_{x'}$ and λ determine its size and degree of anisotropy, W and H are the width and the height of the image to be filtered and finally $\eta_i = (\eta_x, \eta_y)$ is the frequency of the complex sinusoid. If one takes $\sigma_{x'}$ to be Q times the period of the frequency, we get bank of filters governed by 5 parameters, namely $\wp = \{\phi, Q, \lambda, \eta_x, \eta_y\}$. We have tuned 4 different families of Gabor filters. They result when considering the 3 levels in which the left ventricle's short axis view is divided: Base, Mid and Apex; and the long axis view (see figure 2).

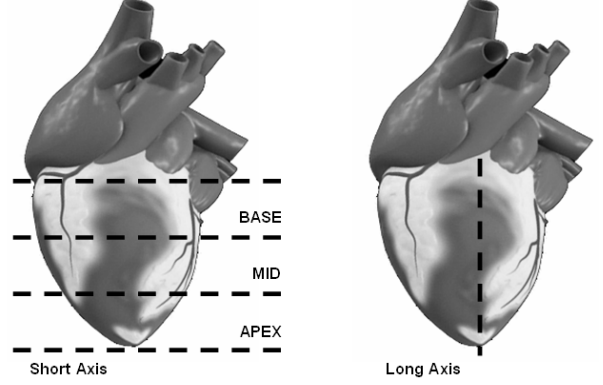


Figure 2: The 2 main views of the left ventricle. Short Axis and the three levels in which is divided: Base, Mid and Apex (left); and Long Axis (right).

The I_k 's, $k = \{1, 2\}$ are given by assigning to each pixel, the maximum response of the bank of filters:

$$I_k(x, y; t) = I(x, y; t) * \Gamma_{\wp_i} \quad (6)$$

with $\|I(x, y; t) * \Gamma_{\wp_i}\| > \|I(x, y; t) * \Gamma_{\wp_j}\|$, $\forall \wp_i \neq \wp_j$, and $\wp_i, \wp_j \in \wp$. Having the I_k 's, its true phase Φ_k cannot be retrieved, but only its wrapped version a_k . Nevertheless, this is not a big problem. If we have a look at equation (3), we realize that this method only uses the spatio-temporal derivatives of the target sequence, in our case, $\Phi_k(x, y; t)$. Taking advantage of the following identity, $\Phi_k = \Im\{\log(I_k)\}$, we can obtain its spatio-temporal derivatives without wrapping effect as:

$$\Phi_{k\ell} = \frac{\left[\Re(\Phi_k) \frac{\partial \Im(\Phi_k)}{\partial \ell} - \Im(\Phi_k) \frac{\partial \Re(\Phi_k)}{\partial \ell} \right]}{\|\Phi_k\|^2} \quad (7)$$

where $\ell = \{x, y, t\}$ and $\Phi_{k\ell} = \frac{\partial \Phi_k}{\partial \ell}$.

Notice that now, the equation (3) becomes a fully determined system:

$$\begin{cases} \varepsilon_1 \equiv \nabla \Phi_1 \cdot V + \Phi_{1t} = 0 \\ \varepsilon_2 \equiv \nabla \Phi_2 \cdot V + \Phi_{2t} = 0 \end{cases}$$

Although we could solve this system for each point, thermal noise and other undesirable artifacts could lead to discontinuous deformation maps, as shown in figure 4.b. For this reason we adopt a regularization scheme in the fashion of (4) using two data terms instead of just one, and a variable weighting function

in order to obtain smooth deformation maps where noise or artifacts are predominant while maintaining original data otherwise:

$$\varepsilon = \int \int \alpha^2 \varepsilon_{reg}^2 + (1 - \alpha)^2 [\varepsilon_1^2 + \varepsilon_2^2] dx dy \quad (8)$$

where α (Fig. 3) is designed to take values in $[0, 1]$:

$$\alpha(x, y) = 1 - \frac{\left[\left(\frac{\|I_1\|}{\max\{\|I_1\|\}} \right) + \left(\frac{\|I_2\|}{\max\{\|I_2\|\}} \right) \right]}{2} \quad (9)$$

Using the calculus of variations, we obtain:

$$\begin{aligned} K [A_{11}u + A_{12}v + A_{13}] &= \dots \\ \dots 2\alpha(\alpha_x u_x + \alpha_y u_y) + \nabla^2 u & \end{aligned} \quad (10)$$

$$\begin{aligned} K [A_{21}u + A_{22}v + A_{23}] &= \dots \\ \dots 2\alpha(\alpha_x v_x + \alpha_y v_y) + \nabla^2 v & \end{aligned}$$

where $K = (1 - \alpha)^2$, ∇^2 is the Laplacian operator and

$$\begin{aligned} A_{11} &= (\Phi_{1x}^2 + \Phi_{2x}^2) \\ A_{12} &= (\Phi_{1x}\Phi_{1y} + \Phi_{2x}\Phi_{2y}) \\ A_{13} &= (\Phi_{1x}\Phi_{1t} + \Phi_{2x}\Phi_{2t}) \\ A_{21} &= A_{12} \\ A_{22} &= (\Phi_{1y}^2 + \Phi_{2y}^2) \\ A_{23} &= (\Phi_{1y}\Phi_{1t} + \Phi_{2y}\Phi_{2t}) \end{aligned}$$

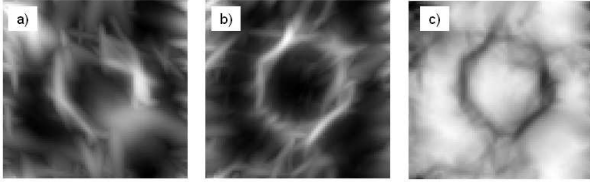


Figure 3: a) $\|\Phi_1\|$, b) $\|\Phi_2\|$ and c) the weighting function derived from them $\alpha(x, y)$.

The solution of this Euler-Lagrange equation (10) is the smooth deformation map that we call *Harmonic Phase Flow* (HPF). Figure 4.e.f shows its performance in front of the previously explained methods.

5 Results

In order to evaluate the precision of our method, we have tested its performance at the Base, Mid and Apex levels from short axis view, and long axis. The

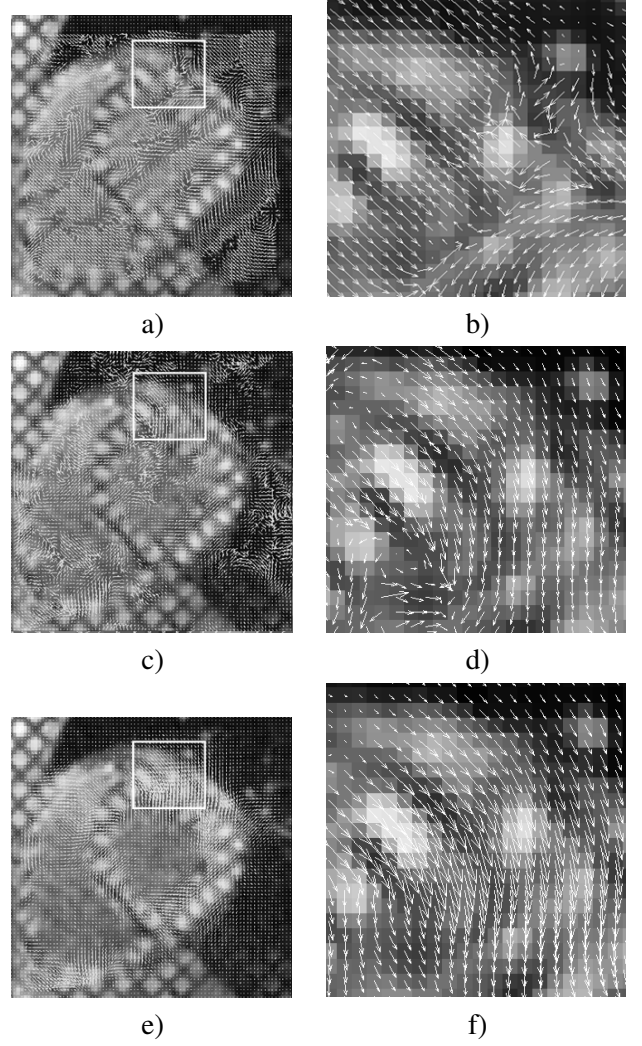


Figure 4: Estimated deformation map for a) HARP image + HARP-tracking, c) Gabor filters + independent estimation and e) Gabor filters + variational framework (HPF), in a mid-systolic basal frame and their respective detail b), d) and f).

reason for doing this is that the three levels and both views present different shape and motion properties. For instance, basal planes suffer from through-plane motion, while apical ones remain almost still. Another example is that apical and basal planes experiment significant rotational motion contrarily to mid ones where radial contraction is predominant. We also divided the systolic cycle in 4 time segments because the deformation of tissue becomes larger as systole evolves. We took 5 Tagged MR sequences for each level and 5 for long axis belonging to different patients and, at each frame, we marked an uniformly spread set of points inside the myocardium. An ex-

pert was asked to manually actualize these points and results were compared to those provided by our method. Mean error is plotted in figure 5.top.

We have applied the *Harmonic Phase Flow* method to the calculation of systolic myocardial rotation over 8 different healthy volunteers (5 men, age: 27 ± 1), which studies were composed by 8 short axis tagged sequences acquired by a Siemens Avanto 1.5T MR scanner.

Rotational data was obtained taking as reference the initial time of systole, and taking into account the centroid of the left ventricle at each frame. From basal-most and apical-most rotation data, we derived the ventricular torsion as the difference of them. Mean obtained results (Fig. 5.bottom), show that during the first 20% of systole, all myocardial levels experiment a counterclockwise rotation (seen from apex to base) that ranges from 1.33° at base, to 4.07° at apex (torsion: 2.74°). After this point, base changes to clockwise rotation and reaches -3.58° , while apex continues to 11.78° , at 90% of systole (torsion: 15.35°). Next, both base and apex change their rotation direction and at end-systole, their values are -3.54° and 11.06° for base and apex respectively (torsion: 14.61°).

These results are consistent to those obtained by manually selecting points in [16]. This fact encourages the use of ventricular torsion as useful parameter for ventricular function assessment in clinical routine.

In figure 6, we show the performance of HPF-based tissue tracking, either in short as in long axis views.

6 Discussion and conclusions

The key idea behind the method we developed here relies on the fact that, although phase images derived from tagged sequences are impossible to obtain without wrapping artifacts, we can track phase values anyway due to the fact that we employ a method that uses their spatio-temporal derivatives only. We have obtained precise phase sequences using bank of Gabor filters, which have been tuned in order to fit tissue shape and adapt to its motion at each left ventricle level and view. We have mixed all these concepts in a variational framework where a variable weighting function has allowed to find, at each point, a proper tradeoff between smoothness and the ground truth.

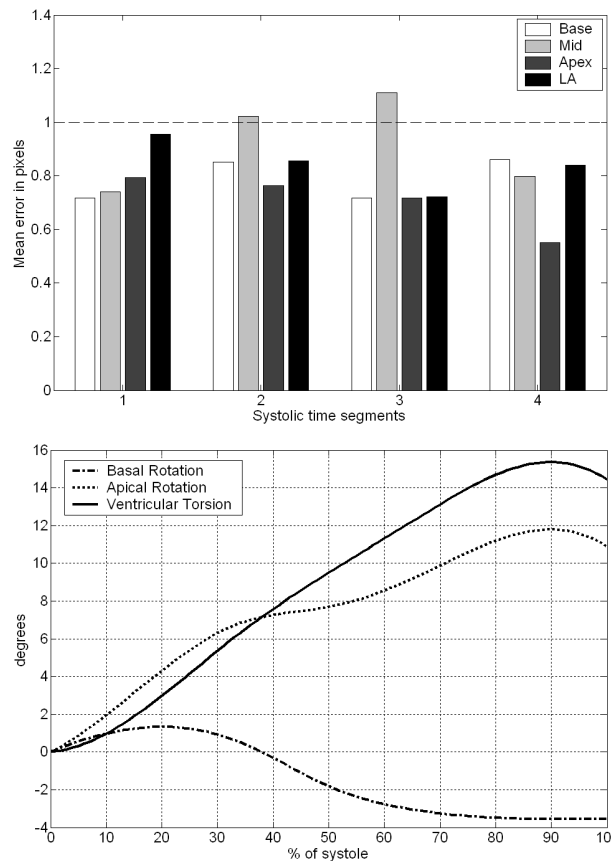


Figure 5: Top: Mean error in pixels for Basal, Mid and Apical levels of short axis view, and long axis. They are grouped in 4 time segments of systole: 0-25%, 25-50%, 50-75% and 75-100%. Bottom: Mean basal and apical rotation, and torsion in systole.

This leads to fully regular deformation maps that extend the tissue motion to zones that would be discontinuous otherwise.

Acknowledgements

This work was supported in part by a research grant from projects FIS-G03/1085, FIS-PI031488, TIC2003-00654 and MI-1509/2005.

References

- [1] Torrent-Guasp F, Ballester M, Buckberg G, Carreras F, Flotats A, Carrió I, Ferreira A, Samuels L, Narula J. Spatial orientation of the ventricular muscle band: physiologic contribu-

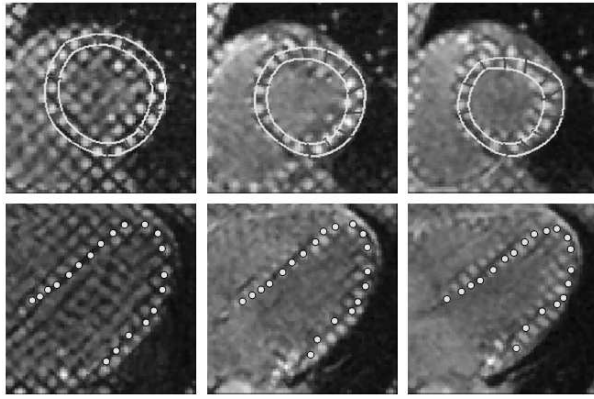


Figure 6: HPF-based tracking in a basal short axis sequence (top) and a long axis sequence (bottom). First column belongs to initial systole, second to mid-systole and last to end-systole.

- tion and surgical implications. *J Thorac Cardiovasc Surg* 2001;122:389–392.
- [2] Axel L, Dougherty L. Mr imaging of motion with spatial modulation of magnetization. *Radiology* 1989;171:841–845.
- [3] Guttman M, Prince J, McVeigh E. Tag and contour detection in tagged mr images of the left ventricle. *IEEE Trans Med Im* 1989;13:74–88.
- [4] Quian Z, Montillo A, Metaxas D, Axel L. Segmenting cardiac mri tagging lines using gabor filter banks. In *Proceedings of International Conference of the Engineering in Medicine and Biology Society*. 2003; 630–633.
- [5] Denney T, Prince J. Optimal brightness functions for optical flow estimation of deformable motion. *IEEE Trans Imag Proc* 1994;3:178–191.
- [6] Dougherty L, Asmuth J, Blom A, Axel L, Kumar R. Validation of an optical flow method for tag displacement estimation. *IEEE Transactions on Medical Imaging* 1999;18:359–263.
- [7] Prince JL, McVeigh ER. Motion estimation from tagged mr images. *IEEE Transactions on Medical Imaging* 1992;11:238–249.
- [8] Osman NF, McVeigh ER, Prince JL. Imaging heart motion using harmonic phase mri. *IEEE Transactions on Medical Imaging* 2000; 19:186–202.
- [9] Kraitchman D, Young A, Chang C, Axel L. Semiautomated tracking of myocardial motion in mr tagged images. *IEEE Transactions on Medical Imaging* 2000;14:422–433.
- [10] Deng X, Denney T. Rapid 3d lv strain reconstruction from tagged cardiac mr images. In *Proceedings of ISMRM*, volume 11. 2003; .
- [11] Osman N, Prince J. On the design of the band-pass filters in harmonic phase mri. In *Proc. of International Conference on Image Processing*, volume 1. 2000; 625–628.
- [12] Montillo A, Metaxas D, Axel L. Extracting tissue deformation using gabor filter banks. In *Proceedings of SPIE*, volume 5369. 2004; 1–9.
- [13] Barajas J, Garcia-Barnes J, Carreras F, Pujadas S, Radeva P. Angle images using gabor filters in cardiac tagged mri. In *Artificial Intelligence Research and Development*, volume 131. 2005; 107–114.
- [14] Osman NF, Kerwin WS, McVeigh ER, Prince JL. Cardiac motion tracking using cine harmonic phase (harp) magnetic resonance imaging. *Magnetic Resonance in Medicine* 1999; 42:1048–1060.
- [15] Horn B, Schunck B. Determining optical flow. *Artificial Intelligence* 1981;17:185–204.
- [16] Lorenz C, Pastorek J, Bundy J. Delineation of normal human left ventricular twist throughout systole by tagged cine magnetic resonance imaging. *J Cardiovasc Magn Reson* 2000; 2(2):97–108.